Gas phase anion photoelectron spectroscopy and theoretical investigation of gold acetylide species

Peng Wang,[1,2] Wenjing Zhang,[1,2] Xi-Ling Xu,[1,2] Jinyun Yuan,[1,3,a)] Hong-Guang Xu,[1,2,a)] and Weijun Zheng[1,2]

[1]*Beijing National Laboratory for Molecular Sciences, State Key Laboratory of Molecular Reaction Dynamics, Institute of Chemistry, Chinese Academy of Sciences, Beijing 100190, China*
[2]*University of Chinese Academy of Sciences, Beijing 100049, People's Republic of China*
[3]*Institute of Nanostructured Functional Materials, Huanghe Science and Technology College, Zhengzhou, Henan 450006, China*

(Received 31 March 2017; accepted 28 April 2017; published online 15 May 2017)

We conducted gas phase anion photoelectron spectroscopy and density functional theory studies on a number of gold acetylide species, such as AuC_2H, AuC_2Au, and Au_2C_2H. Based on the photoelectron spectra, the electron affinities of AuC_2H, AuC_2Au, and Au_2C_2H are measured to be 1.54(±0.04), 1.60(±0.08), and 4.23(±0.08) eV, respectively. The highest occupied molecular orbital–lowest unoccupied molecular orbital (HOMO-LUMO) gaps of AuC_2H and AuC_2Au are measured to be about 2.62 and 2.48 eV, respectively. It is interesting that photoelectron spectra of AuC_2H^- and AuC_2Au^- display similar spectral features. The comparison of experimental and theoretical results confirms that the ground-state structures of AuC_2H^-, AuC_2Au^-, and their neutrals are all linear with Au—C≡C—H and Au—C≡C—Au configurations. The similar geometric structures, spectral features, HOMO-LUMO gaps, and chemical bonding between $AuC_2H^{-/0}$ and $AuC_2Au^{-/0}$ demonstrate that Au atom behaves like H atom in these species. The photoelectron spectrum of $Au_2C_2H^-$ shows that Au_2C_2H has a high electron affinity of 4.23(±0.08) eV, indicating Au_2C_2H is a superhalogen. Further, we found an unusual similarity between the terminal Au atom of $Au_2C_2H^-$ and the iodine atom of $IAuC_2H^-$. *Published by AIP Publishing.* [http://dx.doi.org/10.1063/1.4983304]

I. INTRODUCTION

Metal-acetylide complexes play important roles as reagents or intermediates in organometallic reactions.[1–8] Coinage-metal acetylides such as copper acetylide, silver acetylide, and gold acetylide were synthesized more than a hundred years ago.[9] They have potential applications in the processes of nanowire construction and new materials' synthesis[10–13] although they are explosive.

Gold can, on the one hand, act as a pseudohalogen to form auride compounds when interacting with low electronegativity species, on the other hand, it plays a role similar to hydrogen when interacting with high electronegativity species.[14,15] It is interesting that gold behaves like an H atom sometimes and like a pseudohalogen sometimes because H and halogen are very different in the periodic table. Gold can react with unsaturated hydrocarbon compounds such as alkynes, alkenes, and allenes to form gold-carbides or gold-carbon hydrides.[16–19] There were a number of experimental and theoretical studies on gold-carbides and gold-carbon hydrides. The structures and bonding properties of Au_nC_2H and Au_nC_2 (n = 1-6) neutral and cationic clusters have been studied by density functional theory (DFT) calculations.[20,21] The rotational constants of AuCCH ($X^1\Sigma^+$) were measured by Fourier-transform microwave (FTMW) spectroscopy.[22] The photoelectron spectra of AuC_2^-,[23,24] AuC_3H^-,[25] and AuC_4H^-[26] as well as those of AuC_n^- and AuC_nH^- (n = 2, 4, and 6)[27] were measured using electron velocity map imaging (VMI) technique. The photoelectron spectra and bonding properties of $LAuC_2H^-$ (L = Cl, I, and C_2H) were investigated using the magnetic-bottle anion photoelectron spectroscopy experiment and theoretical calculations.[28]

We are especially interested in gold acetylides because they have potential applications for non-linear optical materials[29–35] and luminescent devices of sensors.[36–40] Previously, we investigated a number of metal acetylide species such as $Co_nC_2H^-$ (n = 1-5)[41] and $HCo_nC_2H^-$ (n = 1-2).[42] Herein, in order to obtain detailed information about the chemical bonding and electronic properties of gold acetylide species, we conducted gas phase anion photoelectron spectroscopy and density functional theory calculations of AuC_2H^-, AuC_2Au^-, and $Au_2C_2H^-$. Our results reveal large highest occupied molecular orbital–lowest unoccupied molecular orbital (HOMO-LUMO) gaps for AuC_2H and AuC_2Au as well as a very high electron affinity (EA) for Au_2C_2H.

II. EXPERIMENTAL AND THEORETICAL METHODS

A. Experimental methods

The experiment was conducted on a home-built apparatus consisting of a laser vaporization source, a time-of-flight mass spectrometer, and a magnetic-bottle photoelectron

a)Authors to whom correspondence should be addressed. Electronic addresses: yuanjinyun0916@iccas.ac.cn and xuhong@iccas.ac.cn, Tel.: +86 10 62635054, Fax: +86 10 62563167.

spectrometer, which has been described previously.[43] The AuC_2H^-, AuC_2Au^-, and $Au_2C_2H^-$ anions were generated by ablating a rotating and translating gold disk target (13 mm diameter) with the second harmonic of a nanosecond Nd:YAG laser (Continuum Surelite II-10), in a gas mixture of helium and ethylene (ethylene 10%), which was allowed to expand into the laser vaporization source through a pulsed valve (General valve series 9) with ~0.4 MPa backing pressure. The generated anions were mass-analyzed by the time-of-flight mass spectrometer. The AuC_2H^-, AuC_2Au^-, and $Au_2C_2H^-$ anions were mass-selected by a mass-gate, decelerated by a momentum decelerator, and then photodetached by the laser beam of another nanosecond Nd:YAG laser (Continuum Surelite II-10, 532 nm, 266 nm). The photoelectrons were energy-analyzed by the magnetic-bottle photoelectron spectrometer. The photoelectron spectra were calibrated using the spectra of Bi^-, Pb^-, Cu^-, and I^- taken at similar conditions. The resolution of the photoelectron spectrometer was approximately 40 meV at an electron kinetic energy of 1 eV.

B. Theoretical methods

The theoretical calculations were performed using density functional theory (DFT) with PBE1PBE functional[44,45] as implemented in the Gaussian 09 program package.[46] The all-electron aug-cc-pvdz basis set[47,48] was used for the C and H atoms and the aug-cc-pvdz-pp basis set[49] with the efficient core potential (ECP) was used for the Au atom. The harmonic vibrational frequencies were calculated to make sure that the optimized structures are real local minima. The total energies were corrected by the zero-point vibrational energies (ZPEs). We also conducted theoretical calculations using the Becke's three-parameter and Lee-Yang-Parr's gradient-corrected correlation hybrid (B3LYP) functional[50,51] and found that the results from the PBE1PBE functional are in better agreement with the experiments than those from the B3LYP functional. So we mainly present the results from the PBE1PBE functional in this work. The natural bond orbital (NBO) analysis was carried out to explore the bonding details.[52] The electron localization function (ELF) analysis implemented in the Multiwfn software was conducted to distinguish the covalent properties.[53]

The density of states (DOSs) simulation was carried out to assist the assignment of spectral structures generated in the experiments, which is based on the theoretically generalized Koopmans' theorem (GKT).[54,55] In the simulated DOS spectra, the peak of each transition corresponds to the removal of an electron from a specific molecular orbital (MO) of the anion. The details of the simulations have been reported elsewhere.[56]

III. EXPERIMENTAL RESULTS

The photoelectron spectra of AuC_2H^- and AuC_2Au^- recorded with 532 and 266 nm photons are displayed in Figure 1. The 266 nm spectra show spectral features of high electron binding energy (EBE), while the 532 nm spectra give better spectral resolution for the low EBE peaks. The vertical detachment energies (VDEs) and adiabatic detachment energies (ADEs) of these anions evaluated from their photoelectron spectra are listed in Table I. The photoelectron spectra of AuC_2H^- and AuC_2Au^- are very similar to each other, except that the VDE of AuC_2Au^- is slightly higher than that of AuC_2H^-, indicating that AuC_2H and AuC_2Au have similar electronic structures.

The 266 nm spectrum of AuC_2H^- (Figure 1) has a low EBE peak centered at 1.60 eV and a high EBE peak at 4.22 eV. The distance between the high EBE peak and low EBE peak is about 2.62 eV, indicating that neutral AuC_2H has a large gap between its highest occupied molecular orbital (HOMO) and lowest unoccupied molecular orbital (LUMO). It suggests that neutral AuC_2H is a highly stable molecule. In the 532 nm spectrum, the low EBE peak is better resolved, thus, several

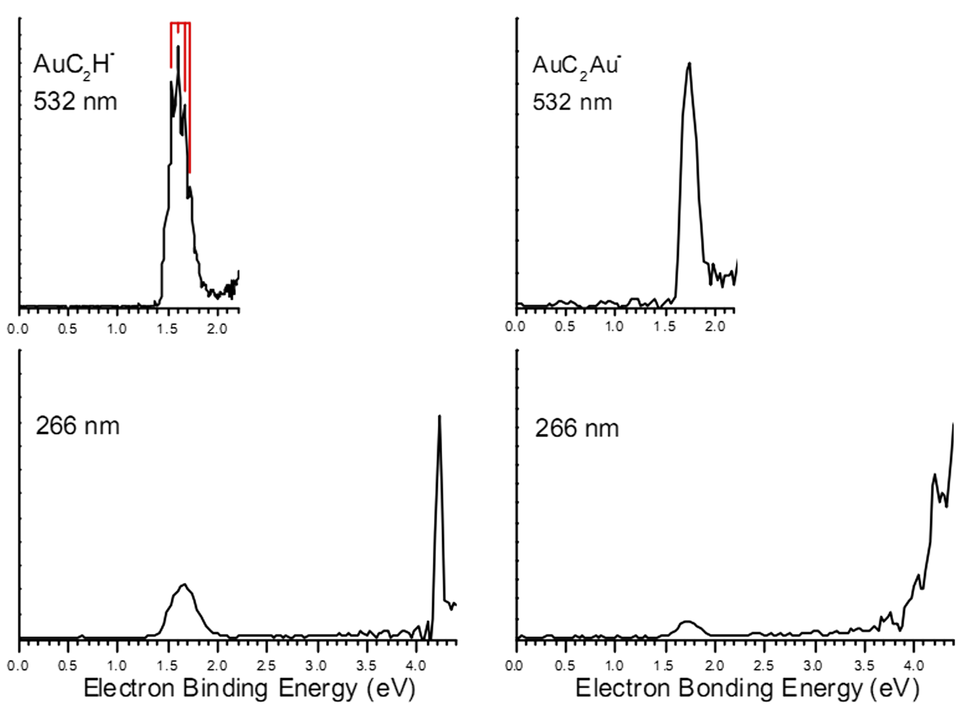

FIG. 1. Photoelectron spectra of AuC_2H^- and AuC_2Au^- obtained with 532 and 266 nm photons. The red vertical lines indicate the resolved vibrational features.

TABLE I. The relative energies, VDEs and ADEs, of the most stable isomers of AuC_2H^-, AuC_2Au^-, and $Au_2C_2H^-$, as well as the comparison of the theoretical VDEs and ADEs with the experimental values.

			VDE (eV)		ADE (eV)	
Isomers	Sym.	State	Theo.	Expt.	Theo.	Expt.
AuC_2H^-	$C_{\infty v}$	$^2\Sigma^+$	1.50	1.60(±0.04)	1.46	1.54(±0.04)
AuC_2Au^-	$D_{\infty h}$	$^2\Sigma_g{}^+$	1.76	1.72(±0.08)	1.73	1.60(±0.08)
$Au_2C_2H^-$	$C_{\infty v}$	$^1\Sigma$	3.94	4.23(±0.08)	3.81	4.14(±0.08)

peaks can be distinguished at 1.54, 1.60, 1.66, and 1.72 eV with spaces of about 0.06 eV (484 ± 50 cm^{-1}), which can be tentatively assigned to the Au—C stretching vibrational mode of neutral AuC_2H, consistent with the value (~445 cm^{-1}) measured using high-resolution photoelectron spectroscopy recently by León *et al.*[27] We can determine the ADE and VDE of AuC_2H^- to be 1.54(±0.04) and 1.60(±0.04) eV, respectively, based on the vibrational resolved peaks. Here, the ADE of AuC_2H^- equals the electron affinity (EA) of its corresponding neutral, AuC_2H. Thus, the EA of AuC_2H is determined to be 1.54 eV.

The 266 nm spectrum of AuC_2Au^- (Figure 1) has a low EBE peak at 1.72 eV and a high EBE at 4.20 eV. Like AuC_2H^-, the distance between the two peaks in the spectrum of AuC_2Au^- indicates that neutral AuC_2Au has a large HOMO-LUMO gap of ~2.48 eV. Due to the low frequency of the Au—C≡C—Au symmetric stretching vibrational mode (which will be confirmed by our theoretical calculations), we were not able to resolve the vibrational peaks in the 532 nm spectrum of AuC_2Au^-. The VDE and ADE of AuC_2Au^- are determined to be 1.72(±0.08) and 1.60(±0.08) eV. The EA of AuC_2Au is determined to be 1.60 eV based on the ADE of AuC_2Au^-.

The photoelectron spectrum of $Au_2C_2H^-$ recorded with 266 nm photons is displayed in Figure 2. The spectrum shows a sharp peak at 4.23 eV, indicating that neutral Au_2C_2H has a high EA of about 4.23 eV.

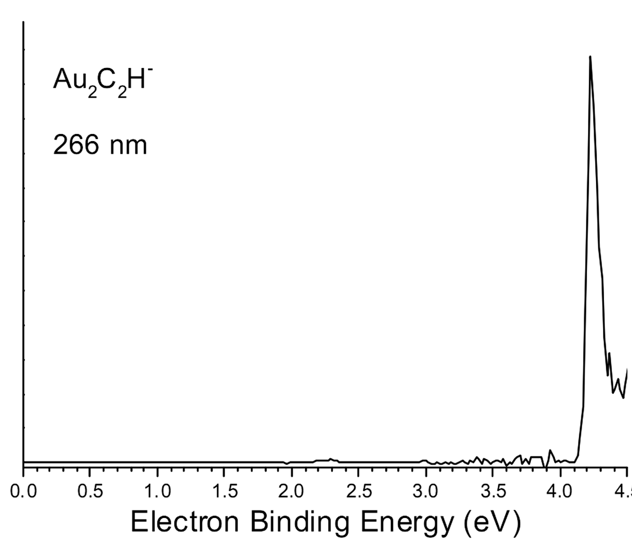

FIG. 2. Photoelectron spectrum of $Au_2C_2H^-$ obtained with 266 nm photons.

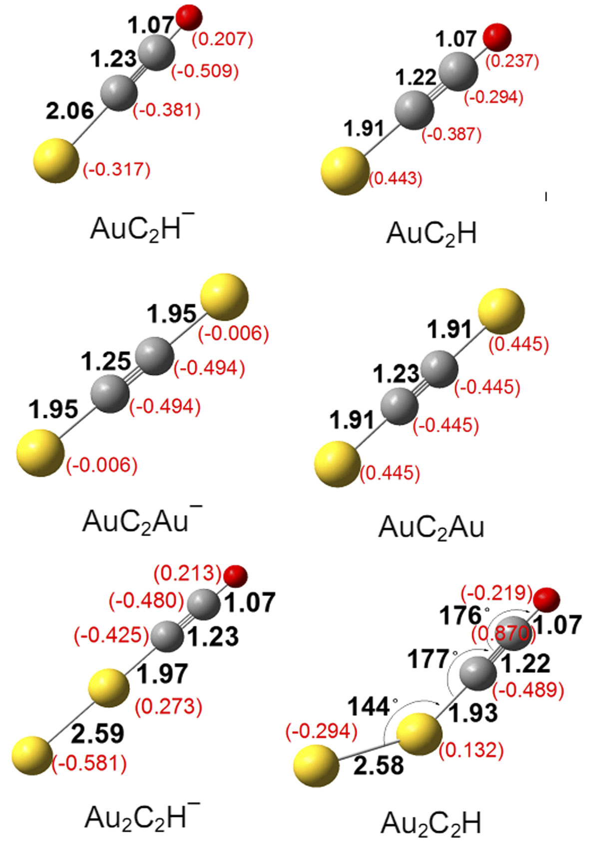

FIG. 3. The most stable structures of $AuC_2H^{-/0}$, $AuC_2Au^{-/0}$, and $Au_2C_2H^{-/0}$. The NPA charges are displayed with the red digits in the parentheses. The unit of bond lengths is Angstrom and that of bond angles is degree.

IV. THEORETICAL RESULTS

Figure 3 shows the most stable isomers of AuC_2H^-, AuC_2Au^-, $Au_2C_2H^-$, and their neutral counterparts. Their theoretical VDEs and ADEs are compared with the experimental values in Table I. Figure 4 displays the comparison of the simulated DOS spectra with the experimental spectra. We have also obtained some other low-lying isomers of AuC_2H^-, AuC_2Au^-, $Au_2C_2H^-$, and their neutral counterparts (supplementary material, Figure S2 and Table S1). Those low-lying isomers are much higher in energy than the most stable ones and their theoretical VDEs also deviate much from our experimental values.

As shown in Figure 3, the theoretical calculations show the most stable isomer of AuC_2H^- to be a linear structure in the $^2\Sigma^+$ electronic state. The Au and H atoms are attached to two terminals of the C≡C, respectively. The Au—C and H—C bond lengths are 2.06 and 1.07 Å, respectively. The C≡C bond length is 1.23 Å, close to that of the acetylene molecule (1.20 Å).[57] The calculated VDE and ADE of isomer 1A are 1.50 and 1.46 eV, respectively, in good agreement with the experimental values (1.60 and 1.54 eV). As shown in Figure 4, the simulated DOS spectrum of most stable isomer of AuC_2H^- reproduces the experimental spectrum very well.

For neutral AuC_2H, the most stable isomer is a linear structure similar to that of AuC_2H^- except for a slightly shorter Au-C bond (1.91 Å). The calculated Au—C (1.91 Å) and C—C (1.22 Å) bond lengths of neutral AuC_2H agree well with the

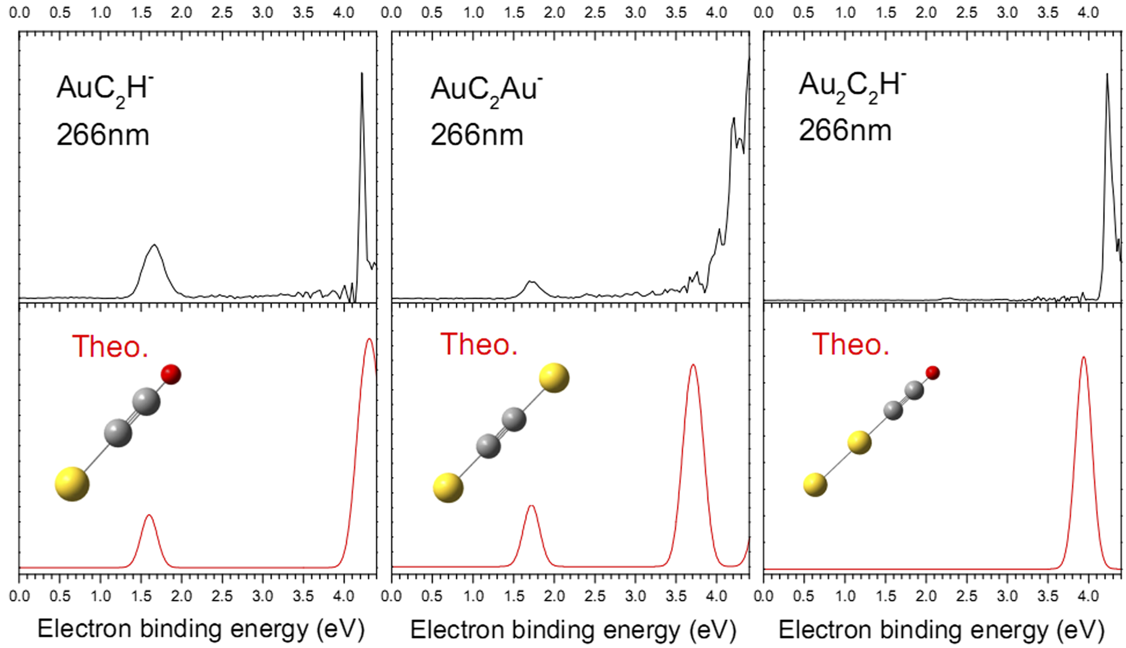

FIG. 4. Comparison of the experimental spectra of AuC_2H^-, AuC_2Au^-, and $Au_2C_2H^-$ with the simulated DOS spectra for their most stable isomers. The simulations were conducted by fitting the distribution of the transition lines with unit-area Gaussian functions of 0.20 eV FWHM (full width at half maximum).

corresponding values (1.93 and 1.21 Å) obtained by Li *et al.*[21] The Au—C bond of neutral AuC_2H is much shorter than that of the AuC_2H^- anion. Thus, the Au—C stretching vibrational mode can be activated upon the detachment of the excess electron from the AuC_2H^- anion. The Au—C stretching vibration frequency of the most stable isomer of neutral AuC_2H is calculated to be 485 cm^{-1}, in excellent agreement with the experimental value (484 ± 50 cm^{-1}) obtained from the 532 nm spectrum of AuC_2H^-.

The most stable isomer of AuC_2Au^- is a linear structure ($D_{\infty h}$, $^2\Sigma_g{}^+$) with the two Au atoms bonded terminally to C≡C, respectively. Its Au—C and C≡C bond lengths are calculated to be 1.95 and 1.25 Å. The calculated VDE and ADE are 1.76 and 1.73 eV, respectively, in good agreement with the experimental values (1.72 and 1.60 eV). The simulated DOS spectrum of most stable isomer of AuC_2Au^- fits the peak positions and patterns of the experimental spectrum very well.

For neutral AuC_2Au, the most stable isomer is linear, similar to the anion global minimum except that it has slightly shorter Au—C (1.91 Å) and C≡C (1.23 Å) bond lengths. Both the Au—C bonds of neutral AuC_2Au are shorter than those of AuC_2Au^- anion. Thus, the Au—C≡C—Au symmetric stretching vibrational mode may be activated upon the detachment of the excess electron from the AuC_2Au^- anion. Our calculations show that the frequency of the Au—C≡C—Au symmetric stretching vibrational mode is about 163 cm^{-1} which is smaller than our photoelectron resolution. That explains why we were not able to resolve the vibrational peaks in the 532 nm spectrum of AuC_2Au^-.

The most stable isomer of $Au_2C_2H^-$ has a linear structure ($C_{\infty v}$, $^1\Sigma$) with the Au_2 unit and H atom bonded terminally to C≡C, respectively. The Au—C and C—H bond lengths are 1.97 Å and 1.23 Å. The C≡C bond length is 1.23 Å, close to that of the acetylene molecule (1.20 Å).[57] The theoretical VDE and ADE are calculated to be 3.94 and 3.81 eV, in good agreement with the experimental values (4.23 and 4.14 eV). The simulated DOS spectrum of most stable isomer of $Au_2C_2H^-$ fits the peak positions and patterns of the experimental spectrum well.

For neutral Au_2C_2H, the most stable isomer has a slightly bent Au—Au—C angle compared to the anion; the Au—C bond and C≡C bonds are shorten to 1.93 Å and 1.22 Å.

V. DISCUSSION

A. Analogy of Au to H in AuCCH$^{-/0}$ and AuCCAu$^{-/0}$

The charge distributions and bonding properties of AuC_2H^-, AuC_2Au^-, and their neutrals were investigated using natural bond orbital (NBO) analyses. The natural charge of each atom is presented in Figure 3, and bond orders of Au—C, C—C bonds are listed in Table II. For AuC_2H^- anion, the natural atomic charge of the Au atom is calculated to be −0.317 e. The NBO analyses indicate that the Wiberg bond order of Au—C bond (WBI_{Au-C}) is 0.66, its covalent percentage is 32%. In contrast with the AuC_2H^- anion, the charge of the

TABLE II. The Au−C and C−C bond orders, Au−C covalent percentages of $AuC_2H^{-/0}$, $AuC_2Au^{-/0}$, and $Au_2C_2H^{-/0}$.

	Wiberg bond order		Laplacian bond order		Covalent percentage
Species	Au—C	C—C	Au—C	C—C	Au—C
AuC_2H^-	0.66	2.91	0.57	2.35	0.32
AuC_2H	0.93	2.93	0.56	2.41	0.59
AuC_2Au^-	0.71	2.94	0.52	2.01	0.60
AuC_2Au	0.93	2.88	0.50	2.12	0.61
$Au_2C_2H^-$	0.61	2.90	0.64	2.36	0.41
Au_2C_2H	0.76	2.88	0.60	2.38	0.65

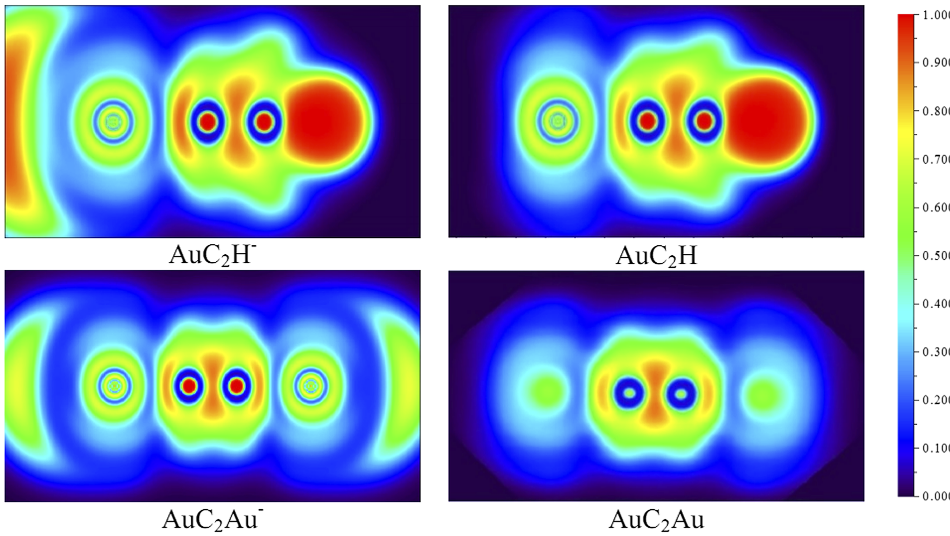

FIG. 5. Electron localization functions analysis of $AuC_2H^{-/0}$ and $AuC_2Au^{-/0}$.

Au atom in neutral AuC_2H is positive (+0.443 e). The Au—C interaction in neutral AuC_2H has more covalent characteristic (59%) than the AuC_2H^- anion, meanwhile the WBI_{Au-C} (0.93) is also larger than that of anionic species. As for anionic and neutral AuC_2Au, the two Au terminals carry the same natural atomic charges of −0.006 e in the AuC_2Au^- anion and +0.445 e in the neutral AuC_2Au, revealing slightly more negative charges on two C atoms than those of $AuC_2H^{-/0}$. The covalent percentages of Au—C interactions for both anionic and neutral AuC_2Au are about 60%with the $WBI_{Au-C} = 0.71$ and 0.93, respectively.

Figure 5 shows the electron localization function (ELF) analyses for $AuC_2H^{-/0}$ and $AuC_2Au^{-/0}$. The ELF reflects the probability to find electron pairs, and larger ELF value means more covalent bonding property. The ELF results demonstrated that the Au—C bond in the AuC_2Au^- anion has obvious probability to find electron pairs than that of in the AuC_2H^- anion, and roughly the same probability in AuC_2H and AuC_2Au neutral. It is also noted that the C—C bond lengths of AuC_2H and AuC_2Au are 1.22 Å and 1.23 Å, respectively, longer than the C≡C bond of acetylene (1.20 Å) and shorter than the C=C bond of ethylene (1.33 Å).[57] The calculated C—C Wiberg bond indexes are in the range of 2.88-2.94, indicating the strong covalent bonding properties of C—C π bonds, which is in agreement with the results of bond lengths and ELF analyses.

To gain insight into the chemical bonding of AuC_2H and AuC_2Au, we also performed systematic molecular orbital (MO) analyses. Figure 6 shows the MO diagram of AuC_2H and AuC_2Au and the comparison of them with those of HC_2H. For AuC_2H, HOMO/-1 describe strong π^* antibonding orbitals, whereas HOMO-5/6 are strong π bonding orbitals. The HOMO-7/8 is a strong Au—C σ bonding orbital. For AuC_2Au, the HOMO/-1 are obvious π^* antibonding orbitals. The HOMO-10/11 and HOMO-12/13 describe strong Au—C π and σ antibonding orbitals, respectively. It is found that the HOMO-5/6 of AuC_2H and the HOMO-10/11 MOs of AuC_2Au are analogous to the HOMO/-1 of C_2H_2, which are all π bonding orbitals. Thus, there is a good correspondence among AuC_2H, AuC_2Au, and HC_2H systems in both MOs and chemical bonding. This study confirms and further extends the analogy between gold and hydrogen in Au—C species.

In organometallic chemistry, the isolable analogy between a gold phosphine unit ($AuPR_3$) and a hydrogen atom has been well recognized in the 1980s,[58,59] and recently Au/H analogy has been found in a number of gas-phase complexes, such as Au—Si,[60–62] Au—B alloy clusters,[63–67] which has been held to originate from the similar electronegativity between Si/B and Au,moreover, the single hydrogen atom in the environment of an Au cluster behaves like the Au atom reported by Ganteför and co-workers.[68] In our experimental spectra of AuC_2H^- and AuC_2Au^-, both of spectral features including VDEs and HOMO-LUMO gaps resemble, implying their electronic structures to be similar. On the other hand, the structure of Au—C≡C—H is linear ($C_{\infty v}$), when hydrogen is replaced by the gold, the structure of Au—C≡C—Au still remains linear ($D_{\infty h}$). The current results strongly support the Au/H analogy in the Au—C cluster systems.

B. Superhalogen property of Au_2C_2H

The sharp high EBE peak in the photoelectron spectrum of $Au_2C_2H^-$ indicates that neutral Au_2C_2H has a very high EA of 4.23(±0.08) eV, which is higher than the EA of the chlorine atom (Cl, 3.61 eV). Therefore, Au_2C_2H can be viewed as a superhalogen.[69] It is interesting to compare $Au_2C_2H^-$ with AuC_2H. Both of them have a linear structure; however, the VDE of AuC_2H^- [1.54(±0.04) eV] is much lower that of $Au_2C_2H^-$. The common-sense explanation is that removing an electron from closed-shell $Au_2C_2H^-$ should be more difficult than from open-shell AuC_2H^-. The orbital interaction diagram of $Au_2C_2H^-$ (Figure 7) can provide more clues for this difference. The HOMO of $Au_2C_2H^-$ mainly consists of the 6s atom orbital (AO) of the terminal Au with minor contribution from HOMO of AuC_2H^-, which is σ^* antibonding orbital with much higher orbital energy. The 6s AO of the terminal Au atom significantly stabilizes the HOMO of $Au_2C_2H^-$. Consequently, the HOMO of $Au_2C_2H^-$ is much lower than that of AuC_2H^- in energy. And the low-lying HOMO in the $Au_2C_2H^-$ anion has increased the electron detachment energy relative to

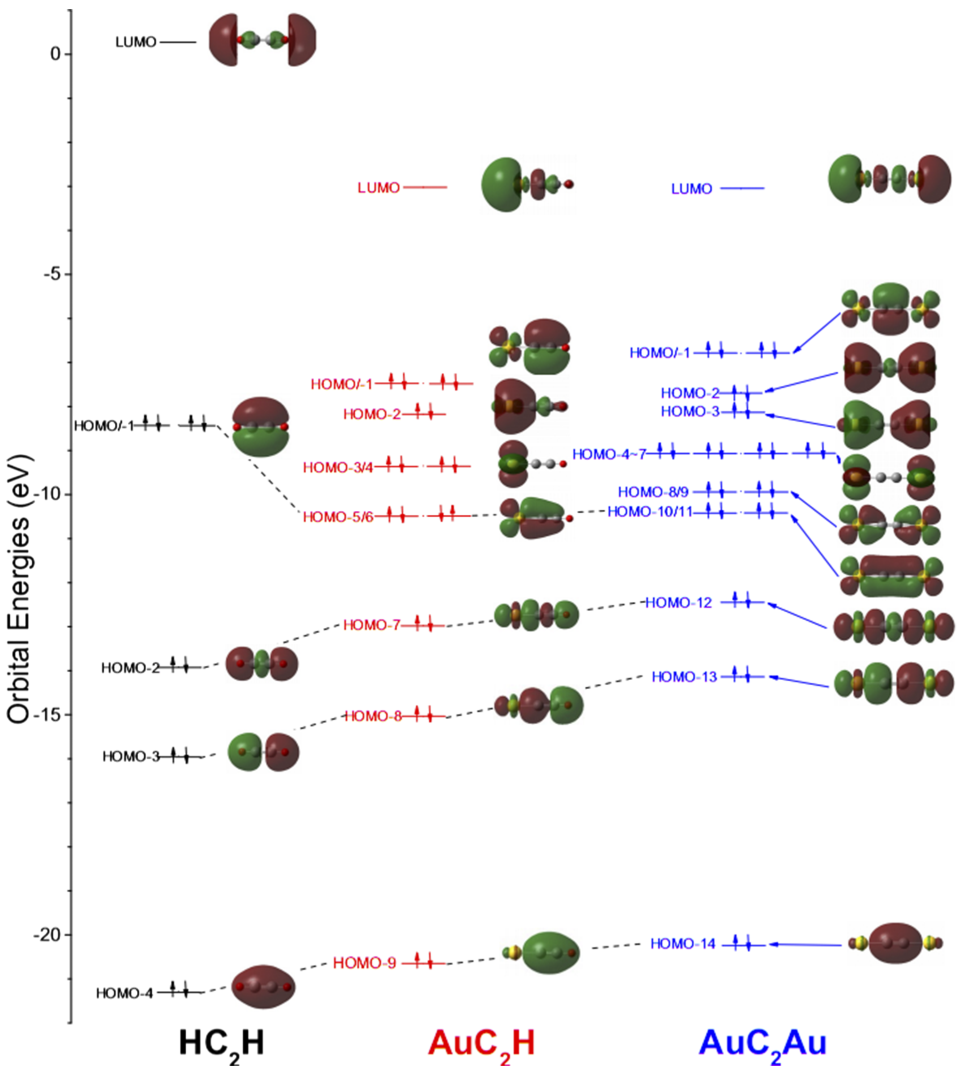

FIG. 6. Comparison of the relevant frontier molecular orbitals of HC_2H, AuC_2H, and AuC_2Au.

the AuC_2H^-. This may explain why $Au_2C_2H^-$ has very high VDE and ADE and its neutral counterpart (Au_2C_2H) has a very high EA. On the other hand, the natural population analysis (NPA) results shown in Figure 3 also can explain this phenomenon. In neutral Au_2C_2H, more positive charge (+0.870 e) is concentrated on the carbon atom beside the hydrogen atom than the central Au atom (+0.132 e), so when we add an extra electron to neutral Au_2C_2H, more extra charge (∼70%) is added on this carbon atom. On the contrast, in the neutral AuC_2H, the extra charge (∼70%) is mainly to be added on the Au atom of AuC_2H with more positive charge (+0.443 e). Comparing the cases of neutral Au_2C_2H and AuC_2H, because of the higher electron affinity of the C_2H unit (2.97 eV)[70] than that of the Au atom (2.31 eV),[71] the extra charge added on the C_2H unit of neutral Au_2C_2H is more stable than that on the Au atom of neutral AuC_2H. That is to explain that the electron affinity of Au_2C_2H is higher than that of AuC_2H.

C. Character of the terminal Au atom in $Au_2C_2H^-$

The Au—C antisymmetric stretching vibrational frequencies of $Au_2C_2H^-$ (446 cm^{-1}) and AuC_2H^- (391 cm^{-1}) and the bond dissociation energy (D_e) of Au—C bonds for $Au_2C_2H^-$ → $Au_2 + C_2H^-$ (D_e = 3.77 eV) and AuC_2H^- → $Au + C_2H^-$ (D_e = 2.50 eV) both suggested that the Au—C bond of $Au_2C_2H^-$ is stronger than that of AuC_2H^-. This fact is also in agreement with the shorter Au—C bond length of $Au_2C_2H^-$ (1.97 Å) than that of $Au_2C_2H^-$ (2.06 Å). These structural features reveal that the terminal Au atom of $Au_2C_2H^-$ significantly strengthens the Au—C bond (isomer 3A), which is because of the *trans*-effect.[72,73] The high electronegative of the terminal Au atom (χp_{Au} = 2.54 eV) polarizes another Au atom of $Au_2C_2H^-$ and enhance the Au—C bond. This *trans*-effect was also observed in $IAuC_2H^-$ by Wang's group, which is caused by terminal iodine (χp_I = 2.66 eV).[28] We optimized the most stable isomer of $IAuC_2H^-$ (shown in Figure S4) using the same function and basis set as those of $Au_2C_2H^-$ and found that the bond lengths of the I—Au (2.62 Å), Au—C (1.96 Å), and C—C (1.23 Å) in $IAuC_2H^-$ are very close to those of $Au_2C_2H^-$ (R_{Au-Au} = 2.59 Å, R_{Au-C} = 1.97 Å, and R_{C-C} = 1.23 Å). The NBO analyses indicated that, for the $Au_2C_2H^-$ anion, the natural atomic charges of the terminal Au atom and central Au atom are −0.581 e and 0.273 e, respectively. Wiberg bond orders of Au—C bond (WBI_{Au-C}) and Au—Au bond (WBI_{Au-Au}) are 0.61 and 0.49, and the covalent percentages of them are 41% and 43%, respectively, while in $IAuC_2H^-$, the

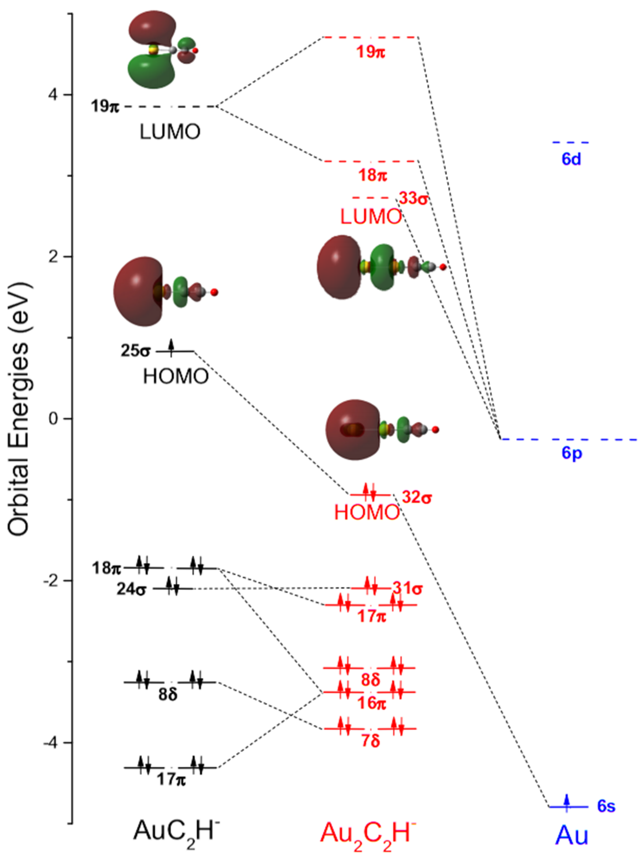

FIG. 7. Orbital interaction diagram of $Au_2C_2H^-$, AuC_2H^-, and Au atom.

I atom and Au atom carry the atom charges of −0.566 e and 0.184 e, respectively, and the covalent percentages of Au—C ($WBI_{Au-C} = 0.64$) and I—Au bond ($WBI_{I-Au} = 0.43$) are 42% and 35%. The above similarities of structural parameters, binding patterns, and charge distributions between $Au_2C_2H^-$ and $IAuC_2H^-$ all show the analogy of gold and iodine. It is probable that the large relativistic effect of Au makes it behaves like hydrogen, but also behaves like the halogen in a few compounds.[74–79]

To further confirm the analogy between the terminal gold of $Au_2C_2H^-$ and iodine of $IAuC_2H^-$, we compared their molecular orbitals. Figure S5 of the supplementary material shows that the bonding of $Au_2C_2H^-$ is quite similar to that of $IAuC_2H^-$. They both have the strong π bonding orbitals (HOMO-8/9 of $IAuC_2H^-$ and HOMO-11/12 of $Au_2C_2H^-$), while the π bonding orbitals are canceled by antibonding π orbitals (HOMO/-1 of $IAuC_2H^-$ and HOMO-1/2 of $Au_2C_2H^-$). Their Au—C bonds are mainly the σ bonding of HOMO-10/11 of $IAuC_2H^-$ and HOMO-13/14 of $Au_2C_2H^-$. In $IAuC_2H^-$, the I—Au bond is from the σ bonding formed by the $5p_z$ orbital of the I atom and the $5d_z{}^2$ orbital of the Au atom (HOMO-5 and HOMO-10). As for $Au_2C_2H^-$, the Au—Au bond also comes from the interaction between the Au $5d_z{}^2$ hybrid orbitals. The remaining orbitals are clearly the gold 5d lone pair or the correspondingly iodine 5p lone pair. Thus, there is a one-to-one correspondence in both the structures and bindings between the $IAuC_2H^-$ and $Au_2C_2H^-$ systems. These results confirmed the analogy of Au in $Au_2C_2H^-$ and I atom in $IAuC_2H^-$.

VI. CONCLUSIONS

In the present work, we performed a combined experimental and theoretical investigation of AuC_2H^-, AuC_2Au^-, and $Au_2C_2H^-$ and their corresponding neutrals. The electron affinities of AuC_2H, AuC_2Au, and Au_2C_2H were estimated to be 1.54(±0.04), 1.60(±0.08), and 4.23(±0.08) eV. Because of the exceptionally high electron affinity of Au_2C_2H, we can consider the Au_2C_2H as a new member of superhalogen. The most stable isomers of AuC_2H^-, AuC_2Au^-, and $Au_2C_2H^-$ were determined by comparing the experimental data to the simulated DOS spectra. The photoelectron spectra revealed the similarity of electronic structures between AuC_2H^- and $Au_2C_2^-$. Meanwhile, the terminal Au atom in the $Au_2C_2H^-$ is similar to that of the I atom in $IAuC_2H^-$ reported in Ref. 28. The charge distribution, chemical bonding, and molecular orbital (MO) analyses demonstrated that both AuC_2H and AuC_2Au have similar electronic and bonding properties, and the similarity also exists between Au_2C_2H and $IAuC_2H$. The current studies further identify the analogies of Au/H in forming novel Au—C clusters and Au/I between $Au_2C_2H^-$ and $IAuC_2H^-$, respectively.

SUPPLEMENTARY MATERIAL

See supplementary material for photoelectron spectrum of $AuC_2{}^-$ with 266 nm photons; low-lying isomers of $AuC2H^{-/0}$, $AuC2Au^{-/0}$, and $Au2C2H^{-/0}$; comparison of the experimental spectra of AuC_2H^-, AuC_2Au^-, and $Au_2C_2H^-$ with their simulated DOS spectra; comparison of most stable isomer of $Au_2C_2H^-$ and $IAuC_2H^-$; comparison of the major bonding orbitals of $IAuC_2H^-$ and $Au_2C_2H^-$; the other details of gold acetylides anions; the theoretical results based on other functions and basis sets; and Cartesian coordinates for stable isomers of $AuC_2H^{0/-}$, $Au_2C_2{}^{0/-}$, and $Au_2C_2H^{0/-}$.

ACKNOWLEDGMENTS

This work was supported by the Natural Science Foundation of China (Grant No. 21401064), the Chinese Academy of Sciences (Grant No. QYZDB-SSW-SLH024), and Beijing National Laboratory for Molecular Sciences (Grant No. 20140164). The theoretical calculations were conducted on the ScGrid of the Supercomputing Center, Computer Network Information Center of the Chinese Academy of Sciences.

[1] R. D. Stephens and C. E. Castro, J. Org. Chem. **28**, 3313–3315 (1963).
[2] C. E. Castro, R. Havlin, V. K. Honwad, A. M. Malte, and S. W. Moje, J. Am. Chem. Soc. **91**, 6464–6470 (1969).
[3] P. Bertus, F. Fecourt, C. Bauder, and P. Pale, New J. Chem. **28**, 12–14 (2004).
[4] R. H. Pouwer, J. B. Harper, K. Vyakaranam, J. Michl, C. M. Williams, C. H. Jessen, and P. V. Bernhardt, Eur. J. Org. Chem. **2007**, 241–248.
[5] R. H. Pouwer, C. M. Williams, A. L. Raine, and J. B. Harper, Org. Lett. **7**, 1323–1325 (2005).
[6] P. Siemsen, R. C. Livingston, and F. Diederich, Angew. Chem., Int. Ed. **39**, 2632–2657 (2000).
[7] A. Simonneau, F. Jaroschik, D. Lesage, M. Karanik, R. Guillot, M. Malacria, J.-C. Tabet, J.-P. Goddard, L. Fensterbank, V. Gandon, and Y. Gimbert, Chem. Sci. **2**, 2417–2422 (2011).
[8] F. Han, J. Li, H. Zhang, T. Wang, Z. Lin, and H. Xia, Chem. - Eur. J. **21**, 565–567 (2015).
[9] J. A. Mathews and L. L. Watters, J. Am. Chem. Soc. **22**, 108–111 (1900).
[10] K. Judai, J. Nishijo, and N. Nishi, Adv. Mater. **18**, 2842–2846 (2006).
[11] F. Cataldo and D. Capitani, Mater. Chem. Phys. **59**, 225–231 (1999).

[12]C.-P. Cho and T.-P. Perng, J. Nanosci. Nanotechnol. **8**, 69–87 (2008).
[13]R. Buschbeck, P. J. Low, and H. Lang, Coord. Chem. Rev. **255**, 241–272 (2011).
[14]P. Pyykkö, Angew. Chem., Int. Ed. **43**, 4412–4456 (2004).
[15]L.-S. Wang, Phys. Chem. Chem. Phys. **12**, 8694–8705 (2010).
[16]A. S. K. Hashmi, Chem. Rev. **107**, 3180–3211 (2007).
[17]Z. Li, C. Brouwer, and C. He, Chem. Rev. **108**, 3239–3265 (2008).
[18]H. Schmidbaur and A. Schier, Organometallics **29**, 2–23 (2010).
[19]A. Corma, A. Leyva-Pérez, and M. J. Sabater, Chem. Rev. **111**, 1657–1712 (2011).
[20]D.-Z. Li and S.-D. Li, J. Cluster Sci. **22**, 331–341 (2011).
[21]D.-Z. Li, M.-Z. Song, Q.-H. Xu, and S.-G. Zhang, J. Cluster Sci. **23**, 481–489 (2012).
[22]T. Okabayashi, H. Kubota, M. Araki, and N. Kuze, Chem. Phys. Lett. **577**, 11–15 (2013).
[23]B. R. Visser, M. A. Addicoat, J. R. Gascooke, W. D. Lawrance, and G. F. Metha, J. Chem. Phys. **138**, 174310 (2013).
[24]I. León, Z. Yang, and L.-S. Wang, J. Chem. Phys. **140**, 084303 (2014).
[25]J.-H. Meng, Q.-Y. Liu, and S.-G. He, J. Phys. Chem. A **119**, 11265–11270 (2015).
[26]B. R. Visser, M. A. Addicoat, J. R. Gascooke, W. D. Lawrance, and G. F. Metha, J. Chem. Phys. **145**, 044320 (2016).
[27]I. Leon, F. Ruiperez, J. M. Ugalde, and L.-S. Wang, J. Chem. Phys. **145**, 064304 (2016).
[28]H.-T. Liu, X.-G. Xiong, P. Diem Dau, Y.-L. Wang, D.-L. Huang, J. Li, and L.-S. Wang, Nat. Commun. **4**, 2201 (2013).
[29]I. R. Whittall, M. G. Humphrey, S. Houbrechts, A. Persoons, and D. C. R. Hockless, Organometallics **15**, 5738–5745 (1996).
[30]R. H. Naulty, M. P. Cifuentes, M. G. Humphrey, S. Houbrechts, C. Boutton, A. Persoons, G. A. Heath, D. C. R. Hockless, B. Luther-Davies, and M. Samoc, J. Chem. Soc., Dalton Trans. **22**, 4167–4174 (1997).
[31]J. Vicente, M. T. Chicote, M. D. Abrisqueta, M. C. Ramírez de Arellano, P. G. Jones, M. G. Humphrey, M. P. Cifuentes, M. Samoc, and B. Luther-Davies, Organometallics **19**, 2968–2974 (2000).
[32]S. K. Hurst, N. T. Lucas, M. G. Humphrey, I. Asselberghs, R. V. Boxel, and A. Persoons, Aust. J. Chem. **54**, 447–451 (2001).
[33]S. K. Hurst, M. P. Cifuentes, A. M. McDonagh, M. G. Humphrey, M. Samoc, B. Luther-Davies, I. Asselberghs, and A. Persoons, J. Organomet. Chem. **642**, 259–267 (2002).
[34]S. K. Hurst, M. G. Humphrey, J. P. Morrall, M. P. Cifuentes, M. Samoc, B. Luther-Davies, G. A. Heath, and A. C. Willis, J. Organomet. Chem. **670**, 56–65 (2003).
[35]C. E. Powell and M. G. Humphrey, Coord. Chem. Rev. **248**, 725–756 (2004).
[36]D. Li, X. Hong, C.-M. Che, W.-C. Lo, and S.-M. Peng, J. Chem. Soc., Dalton Trans. **19**, 2929–2932 (1993).
[37]M. J. Irwin, J. J. Vittal, and R. J. Puddephatt, Organometallics **16**, 3541–3547 (1997).
[38]W. Lu, N. Zhu, and C.-M. Che, J. Organomet. Chem. **670**, 11–16 (2003).
[39]M. C. Blanco, J. Cámara, M. C. Gimeno, P. G. Jones, A. Laguna, J. M. López-de-Luzuriaga, M. E. Olmos, and M. D. Villacampa, Organometallics **31**, 2597–2605 (2012).
[40]A. Leyva-Pérez, A. Doménech-Carbó, and A. Corma, Nat. Commun. **6**, 6703 (2015).
[41]J. Yuan, H.-G. Xu, Z.-G. Zhang, Y. Feng, and W. Zheng, J. Phys. Chem. A **115**, 182–186 (2011).
[42]J. Yuan, G.-L. Hou, B. Yang, H.-G. Xu, and W.-J. Zheng, J. Phys. Chem. A **118**, 6757–6762 (2014).
[43]H.-G. Xu, Z.-G. Zhang, Y. Feng, J. Yuan, Y. Zhao, and W. Zheng, Chem. Phys. Lett. **487**, 204–208 (2010).
[44]J. P. Perdew, M. Ernzerhof, and K. Burke, J. Chem. Phys. **105**, 9982–9985 (1996).
[45]C. Adamo and V. Barone, J. Chem. Phys. **110**, 6158–6170 (1999).
[46]M. J. Frisch, G. W. Trucks, H. B. Schlegel, G. E. Scuseria, M. A. Robb, J. R. Cheeseman, G. Scalmani, V. Barone, G. A. Petersson, H. Nakatsuji, X. Li, M. Caricato, A. Marenich, J. Bloino, B. G. Janesko, R. Gomperts, B. Mennucci, H. P. Hratchian, J. V. Ortiz, A. F. Izmaylov, J. L. Sonnenberg, D. Williams-Young, F. Ding, F. Lipparini, F. Egidi, J. Goings, B. Peng, A. Petrone, T. Henderson, D. Ranasinghe, V. G. Zakrzewski, J. Gao, N. Rega, G. Zheng, W. Liang, M. Hada, M. Ehara, K. Toyota, R. Fukuda, J. Hasegawa, M. Ishida, T. Nakajima, Y. Honda, O. Kitao, H. Nakai, T. Vreven, K. Throssell, J. A. Montgomery, Jr., J. E. Peralta, F. Ogliaro, M. Bearpark, J. J. Heyd, E. Brothers, K. N. Kudin, V. N. Staroverov, T. Keith, R. Kobayashi, J. Normand, K. Raghavachari, A. Rendell, J. C. Burant, S. S. Iyengar, J. Tomasi, M. Cossi, J. M. Millam, M. Klene, C. Adamo, R. Cammi, J. W. Ochterski, R. L. Martin, K. Morokuma, O. Farkas, J. B. Foresman, and D. J. Fox, GAUSSIAN 09, Revision A.02, Gaussian, Inc., Wallingford, CT, 2009.
[47]T. H. Dunning, Jr., J. Chem. Phys. **90**, 1007–1023 (1989).
[48]R. A. Kendall, T. H. Dunning, Jr., and R. J. Harrison, J. Chem. Phys. **96**, 6796–6806 (1992).
[49]K. A. Peterson and C. Puzzarini, Theor. Chem. Acc. **114**, 283–296 (2005).
[50]C. Lee, W. Yang, and R. G. Parr, Phys. Rev. B **37**, 785–789 (1988).
[51]A. D. Becke, J. Chem. Phys. **98**, 5648–5652 (1993).
[52]J. P. Foster and F. Weinhold, J. Am. Chem. Soc. **102**, 7211–7218 (1980).
[53]T. Lu and F. Chen, J. Comput. Chem. **33**, 580–592 (2012).
[54]D. J. Tozer and N. C. Handy, J. Chem. Phys. **109**, 10180–10189 (1998).
[55]J. Akola, M. Manninen, H. Häkkinen, U. Landman, X. Li, and L.-S. Wang, Phys. Rev. B **60**, R11297–R11300 (1999).
[56]X.-L. Xu, X.-J. Deng, H.-G. Xu, and W.-J. Zheng, Phys. Chem. Chem. Phys. **17**, 31011–31022 (2015).
[57]R. J. Berry and M. D. Harmony, Struct. Chem. **1**, 49–59 (1990).
[58]J. W. Lauher and K. Wald, J. Am. Chem. Soc. **103**, 7648–7650 (1981).
[59]F. Scherbaum, A. Grohmann, G. Müller, and H. Schmidbaur, Angew. Chem., Int. Ed. **28**, 463–465 (1989).
[60]B. Kiran, X. Li, H. J. Zhai, L. F. Cui, and L. S. Wang, Angew. Chem., Int. Ed. **43**, 2125–2129 (2004).
[61]X. Li, B. Kiran, and L.-S. Wang, J. Phys. Chem. A **109**, 4366–4374 (2005).
[62]B. Kiran, X. Li, H.-J. Zhai, and L.-S. Wang, J. Chem. Phys. **125**, 133204 (2006).
[63]H. Bai, H.-J. Zhai, S.-D. Li, and L.-S. Wang, Phys. Chem. Chem. Phys. **15**, 9646–9653 (2013).
[64]Q. Chen, H. Bai, H.-J. Zhai, S.-D. Li, and L.-S. Wang, J. Chem. Phys. **139**, 044308 (2013).
[65]Q. Chen, H.-J. Zhai, S.-D. Li, and L.-S. Wang, J. Chem. Phys. **138**, 084306 (2013).
[66]T. K. Ghanty, J. Chem. Phys. **123**, 241101 (2005).
[67]W.-Z. Yao, D.-Z. Li, and S.-D. Li, J. Comput. Chem. **32**, 218–225 (2011).
[68]S. Buckart, G. Ganteför, Y. D. Kim, and P. Jena, J. Am. Chem. Soc. **125**, 14205–14209 (2003).
[69]G. L. Gutsev and A. I. Boldyrev, Chem. Phys. **56**, 277–283 (1981).
[70]K. M. Ervin and W. C. Lineberger, J. Chem. Phys. **95**, 1167–1177 (1991).
[71]H. Hotop and W. C. Lineberger, J. Phys. Chem. Ref. Data **14**, 731–750 (1985).
[72]M. Palusiak, C. F. Guerra, and F. M. Bickelhaupt, Int. J. Quantum Chem. **109**, 2507–2519 (2009).
[73]A. Y. Sokolov and O. V. Sizova, Russ. J. Gen. Chem. **80**, 1223–1231 (2010).
[74]P. Pyykkö, Angew. Chem., Int. Ed. **41**, 3573–3578 (2002).
[75]A. V. Mudring, M. Jansen, J. Daniels, S. Krämer, M. Mehring, J. P. P. Ramalho, A. H. Romero, and M. Parrinello, Angew. Chem., Int. Ed. **41**, 120–124 (2002).
[76]L. Gagliardi, J. Am. Chem. Soc. **125**, 7504–7505 (2003).
[77]L. Gagliardi and P. Pyykko, Phys. Chem. Chem. Phys. **6**, 2904–2906 (2004).
[78]T. K. Ghanty, K. R. S. Chandrakumar, and S. K. Ghosh, J. Chem. Phys. **120**, 11363–11366 (2004).
[79]Y. Erdogdu, T. Jian, G. V. Lopez, W.-L. Li, and L.-S. Wang, Chem. Phys. Lett. **610–611**, 23–28 (2014).